Electronic supplementary information for

Lead-free Mn-doped antimony halide perovskite quantum dots with bright deep-red emission

Aifei Wang, [‡a,b] Faheem Muhammad, [‡a] Yao Liu,[a] and Zhengtao Deng*[a]

a. *College of Engineering and Applied Sciences, State Key Laboratory of Analytical Chemistry for Life Science, National Laboratory of Microstructures, Nanjing University, Nanjing, Jiangsu, 210023, P. R. China*

b. *Current address：Institute of Advanced Materials (IAM), Nanjing Tech University (NJ Tech), 5 Xinmofan Road, Nanjing 210009, P.R. China*

EXPERIMENTAL SECTION

Chemicals. All reagents and solvents were used without further purification. Antimony trichloride ($SbCl_3$, 99.95 %), antimony tribromide ($SbBr_3$, 99.5 %, alfa), Magnesium chloride hexahydrate (MgCl2·6H2O, AR, Aladdin), Magnesium bromide hexahydrate ($MgBr_2 \cdot 6H_2O$, 98 %, Aladdin), Manganese chloride ($MnCl_2 \cdot 4H_2O$, 99.0 %, Aladdin), Manganese(II) bromide ($MnBr_2$, 99%, Aladdin), Caesium chloride (CsCl, ≥99 %, Aladdin), Caesium bromide (CsBr, 99.5 %, Aladdin), Oleylamine (OLAm, 80-90%, Aladdin), oleic acid (OA, 85%, Aladdin), Dimethylsulfoxide (DMSO, AR, Xiya), Isopropanol (IPA, AR ≥99.5 %, Macklin), n-Octanoic acid (98 %, Aladdin), poly(ethylene glycol) methyl ether thiol (PEG-SH, Mn=5000, Aldrich), 1-Dodecanethiol (98 %, Aladdin), 1-Octanethiol (98 %, Aladdin), n-Butanol (99 %, Aladdin), 3-Mercaptopropionic acid (MPA, 98%, Aladdin).

Synthesis of Mn^{2+}-doped $Cs_3Sb_2Cl_x/Br_{9-x}$ (0≤x≤9) perovskite quantum dots. Colloidal Mn^{2+}-doped $Cs_3Sb_2X_9$ NCs were synthesized following the ligand-assisted reprecipitation (LARP) technique. Typically, precursor solution was prepared by dissolving a mixture of CsX (0.6 mmol), SbX_3 (0.4 mmol), OLAm (0.3 mmol) into DMSO (4 mL). Then, precursor solution 200 µL was dropped into a clear solution of mixed solution of 2 mL IPA, MnX_2 (0.01-0.1 mmol) and 30 mg poly(ethylene glycol)methyl ether thiol (mPEG-SH,) under vigorous stirring. Claret fluorescence emission was observed during stirring. Different Cl^- and Br^- ratios in Mn^{2+}-doped $Cs_3Sb_2Cl_x/Br_{9-x}$ (0≤x≤ 9) perovskite QDs were tuned by adding additional MgX_2. Ligands effects on Mn^{2+}-doped $Cs_3Sb_2X_9$ NCs were studied by simply substituting the equimolar amounts of organic carboxylic acid or mercaptan (OA, n-Octanoic acid, 1-Dodecanethiol, 1-Octanethiol, n-Butanol, MPA).

Characterization Details. Powder X-ray diffraction (PXRD) was measured with a Bruker AXS D8 X-ray diffractometer equipped with monochromatized Cu Kα radiation (λ=1.5418 Å). Transmission electron microscopy (TEM) was performed on an FEI Tecnai G2 F20 electron microscope operating at 200 kV. Photoluminescence (PL) spectra were obtained with a Horiba PTI QuantaMaster 400 steady-state fluorescence system. The absolute fluorescence quantum yields were measured using a Horiba PTI QuantaMaster 400 steady-state fluorescence system with an integrated sphere and a Quantaurus-QY absolute PL quantum yield spectrometer (C11347 series).

Cell labelling with QDs and Confocal microscopy. Cell lines were cultured in RPMI 1640 medium supplemented with 10% heat-inactivated fetal bovine serum (GIBCO) and 100 units ml-1 penicillin–streptomycin (Cellgro) in a humidified incubator at 37 °C containing 5% CO_2. Cell binding buffer was prepared by dissolving 0.9 g glucose (Sigma), 0.2033 g magnesium chloride hexahydrate (Sigma), 20 mg yeast tRNA (Sigma) and 200 mg BSA in 200 ml 1 Dulbecco's PBS (with $MgCl_2$ and $CaCl_2$) supplemented with 10% FBS (heat inactivated). 1 x 10^5 Ramos cells were suspended in 300 μl buffer containing 200 nM of Mn^{2+}-doped $Cs_3Sb_2Cl_x/Br_{9-x}$ ($0 \le x \le 9$) perovskite QDs and incubated at 4 °C for a few minutes. The cells were then recollected by centrifugation and washed. The images were obtained with a Zeiss LSM 510 confocal microscope.

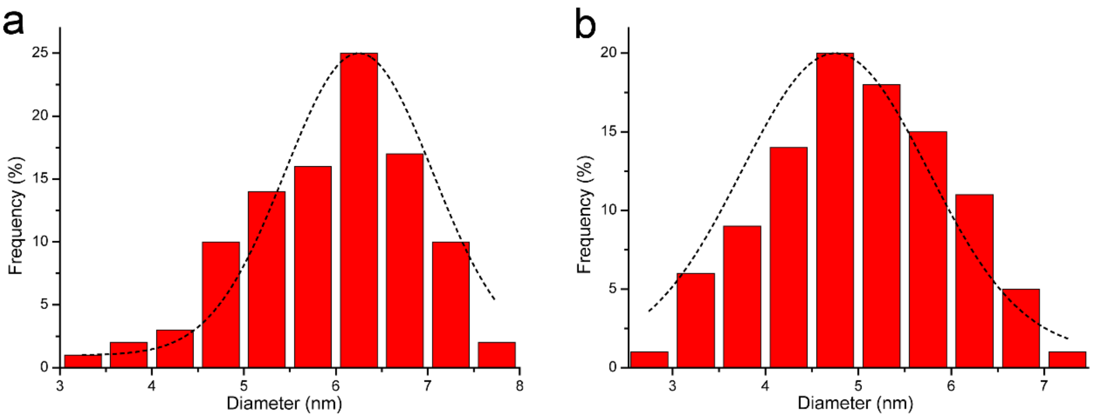

Figure S1. Size distribution histogram of (a) undoped $Cs_3Sb_2Cl_9$ and (b) Mn-doped $Cs_3Sb_2Cl_x/Br_{9-x}$ ($0 \le x \le 9$) QDs.

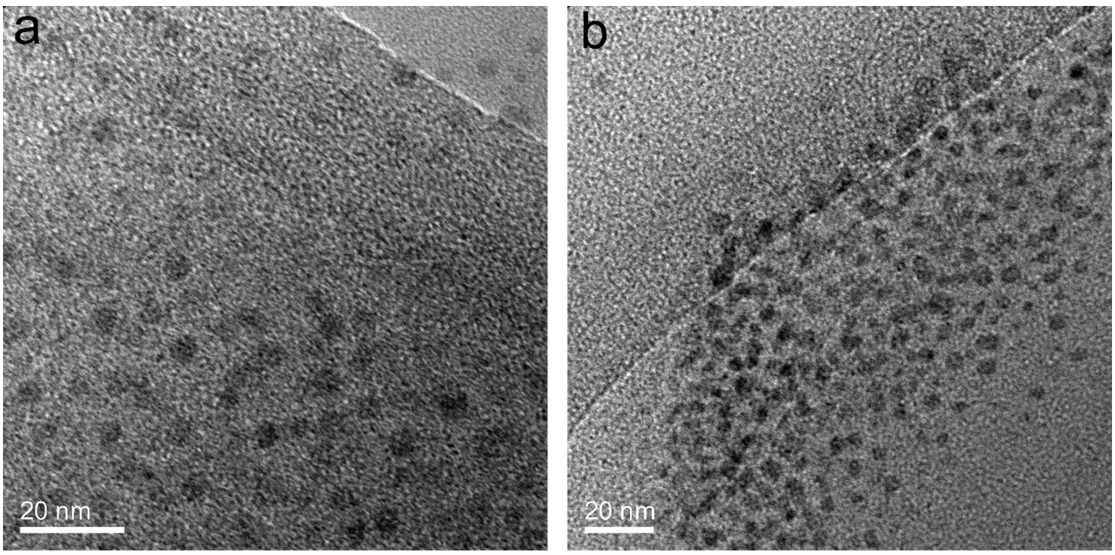

Figure S2. TEM images of other Mn^{2+}-doped $Cs_3Sb_2Cl_x/Br_{9-x}$ ($0 \le x \le 9$) QDs with feeding ratio of (a) Sb: Mn=1:1 and (b) Sb: Mn=1:3.

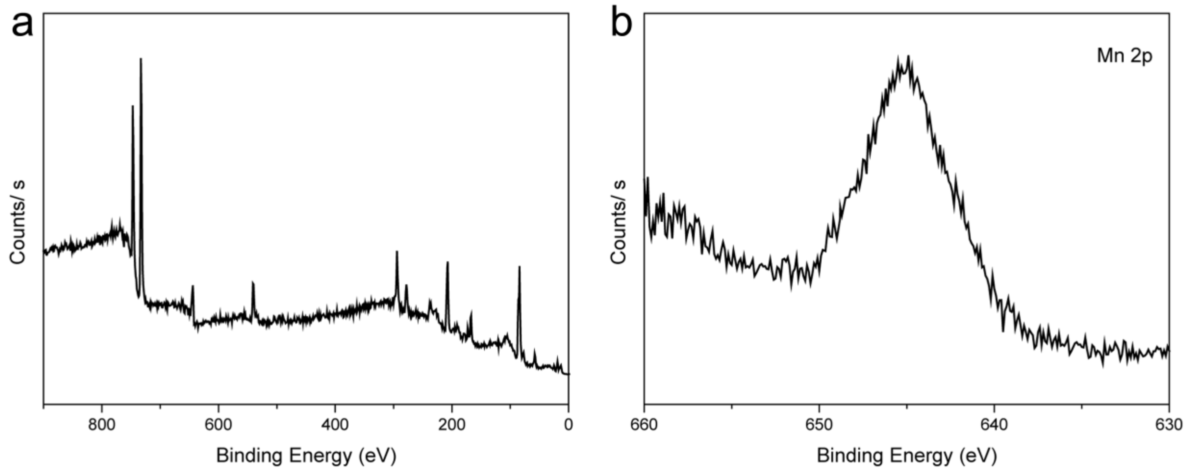

Figure S3. XPS spectra of Mn-doped Cs3Sb2Cl9 and Cs3Sb2Clx/Br9-x (actual feeding ratio of Cl:Br =2:1 and Mn:Sb =2:1) QDs.

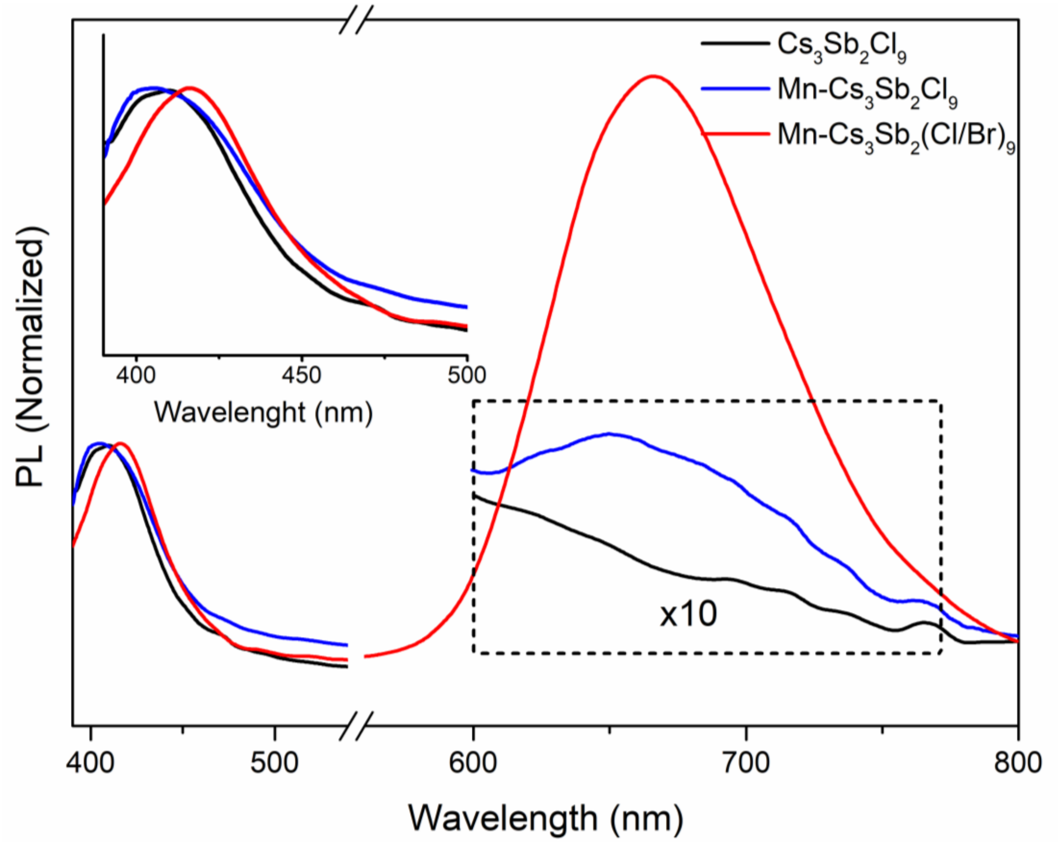

Figure S4. PL emission spectra of the undoped $Cs_3Sb_2Cl_9$, Mn-doped $Cs_3Sb_2Cl_9$ and $Cs_3Sb_2Cl_x/Br_{9-x}$ (actual feeding ratio of Cl:Br =2:1 and Mn:Sb =2:1) QDs.

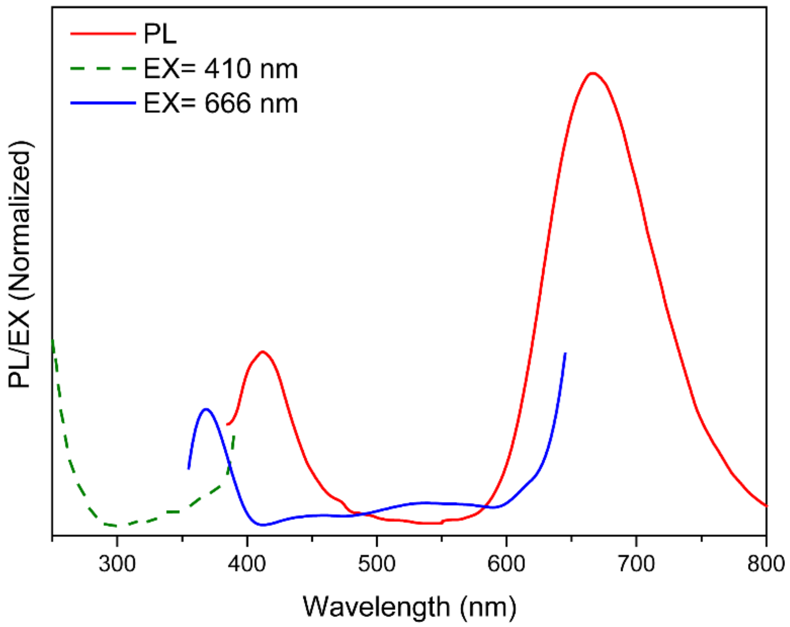

Figure S5. PL excitation (EX) and PL emission spectra of Mn^{2+}-doped $Cs_3Sb_2Cl_x/Br_{9-x}$ ($0 \le x \le 9$) QDs.

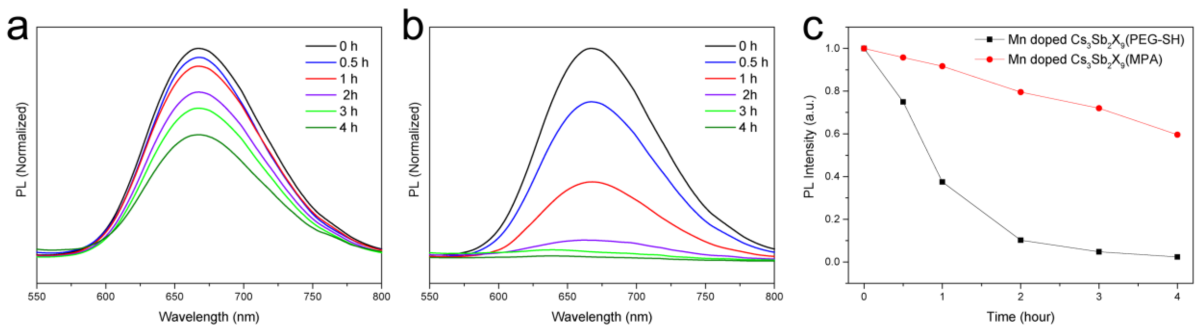

Figure S6. PL intensity changes of the Mn-doped QDs in the presence of water within 4 hours. (a) MPA and (b) PEG-SH synthesized Mn-doped $Cs_3Sb_2(Br_{0.25}/Cl_{0.75})_9$ QDs. (c) summary of the PL intensity changes of (a) and (b).

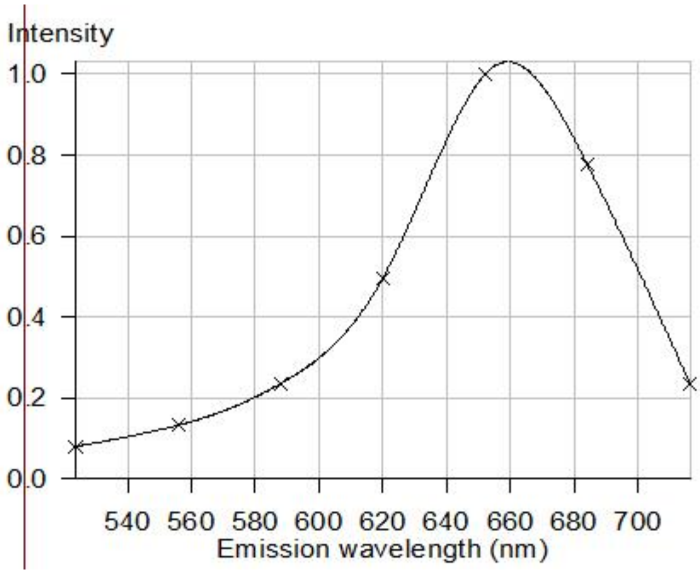

Figure S7. PL emission spectrum of Mn^{2+}-doped $Cs_3Sb_2Cl_x/Br_{9-x}$ (0≤x≤9) QDs labeled on Ramos cells taking with the confocal microscope. The excitation wavelength is 405 nm.

Table S1. Summary of comparison PL characteristics of undoped and Mn^{2+}-doped lead-free halide perovskite materials in bulk and QDs form. High temperature (HT) and room temperature (RT).

Composition	**Sample Size**	**Synthesize Method**	**PL center**	**PL QYs (Measure Method)**	**Ref.**
$Cs_3Sb_2Cl_9$ nanowires	20 nm (diameter)	hot-injection (HT)	436 nm	4% (integrated sphere)	1
$Cs_3Sb_2Br_9$ QDs	3.07 nm	ligand-assisted reprecipitation (RT)	410 nm	46% (standard sample)	2
$Cs_3Bi_2I_9$ NCs	19 nm	hot-injection (HT)	580 - 605 nm	0.017% (not mention)	3
$MA_3Bi_2Br_9$ QDs	3.05 nm	ligand-assisted reprecipitation (RT)	360 - 540 nm	12% (standard sample)	4
$MA_3Bi_2Br_9$ QDs	6.02 nm	ligand-assisted reprecipitation (RT)	422 nm	54.1% (standard sample)	5
$Cs_3Bi_2Br_9$ QDs	6 nm	ligand-assisted reprecipitation (RT)	460 nm	0.2%-4.5% (standard sample)	6
Cs_2AgBiX_6 QDs	8 nm	hot-injection (HT)	629-738 nm	~0.3 ± 0.3% (not meantion)	7
Mn-doped $Cs_2AgInCl_6$	bulk crystals	concentrated acid precipitation	632 nm	doped=3-5% (standard sample)	8

		(RT)			
Mn-doped $Cs_2AgInCl_6$ QDs	9.8 nm (undoped) 12 nm (doped)	hot-injection (HT)	bandadge=560nm doped=620nm	undoped =1.6% doped=16% (integrated sphere)	[9]
Mn-doped $Cs_2NaBiCl_6$	bulk crystals	concentrated acid precipitation (RT)	590 nm	doped=15% (integrated sphere)	[10]
Mn-doped $Cs_2NaBiCl_6$	11 nm	hot-injection (HT)	600 nm	5.0%.	[11]
Mn-Doped $Cs_2NaIn_xBi_{1-x}Cl_6$	10.45 ± 0.5 nm	hot-injection (HT)	around 600 nm	44.6%	[12]
$Cs_3Sb_2Cl_x/Br_{9-x}$ ($0 \le x \le 9$) QDs	6 nm	ligand-assisted reprecipitation (RT)	bandadge=410-465nm doped=660nm	undoped=0.8% doped=49% (integrated sphere)	This work

Table S2. Summary of Mn^{2+} emission lifetime analysis of various feeding molar ratio of Mn/Sb.

Mn:Sb	**τ1**	**τ2**	**A1**	**A2**	**τ ns**
0.5:1	0.78	91.06	11081.71	5356.84	496437.6
1:1	34.85	63.66	1201.85	2246.88	184920.9
2:1	0.78	23.82	16521.21	3013.03	143639.4
3:1	1.46	30.04	4299.52	1817.51	60875.3

Table S3. Summary of Mn^{2+} emission lifetime analysis of various feeding molar ratio of Cl/Br.

Cl Content	**τ1**	**τ2**	**A1**	**A2**	**τ ns**
100 %	1.07	12.43	18442.72	826.03	30001.26
60 %	9.93	54.9	578.96	208.08	17172.66
50 %	1.12	47.63	15820.47	1527.75	90485.66
33 %	1.05	54.67	15767.39	2276.97	141037.7

Table S4. Bond dissociation energy (kJ/mol) of metals cations and halides/ligands anions.

	Cs^+	**Sb^{3+}**	**Mn^{2+}**
Cl^-	117.4	410	337.6
Br^-	610.5	373	323.8
S^{2-}	-	378.7	318

References for supplementary information：

1. B. Pradhan, G. S. Kumar, S. Sain, A. Dalui, U. K. Ghorai, S. K. Pradhan and S. Acharya, *Chem. Mater.*, 2018, **30**, 2135-2142.
2. J. Zhang, Y. Yang, H. Deng, U. Farooq, X. Yang, J. Khan, J. Tang and H. Song, *ACS nano*, 2017, **11**, 9294-9302.
3. Y. Zhang, J. Yin, M. R. Parida, G. H. Ahmed, J. Pan, O. M. Bakr, J. L. Bredas and O. F. Mohammed, *J. Phys. Chem. Lett.*, 2017, **8**, 3173–3177.
4. M. Leng, Z. Chen, Y. Yang, Z. Li, K. Zeng, K. Li, G. Niu, Y. He, Q. Zhou and J. Tang, *Angew. Chem. Int. Ed.*, 2016, **55**, 15012-15016.
5. M. Leng, Y. Yang, Z. Chen, W. Gao, J. Zhang, G. Niu, D. Li, H. Song, J. Zhang, S. Jin and J. Tang, *Nano Lett.*, 2018, **18**, 6076–6083.
6. B. Yang, J. Chen, F. Hong, X. Mao, K. Zheng, S. Yang, Y. Li, T. Pullerits, W. Deng and K. Han, *Angew. Chem.*, 2017, **129**, 12645-12649.
7. S. E. Creutz, E. N. Crites, M. C. De Siena and D. R. Gamelin, *Nano Lett.*, 2018, **18**, 1118-1123.
8. N. N. K and A. Nag, *Chem. Commun.*, 2018, **54**, 5205-5208.
9. F. Locardi, M. Cirignano, D. Baranov, Z. Dang, M. Prato, F. Drago, M. Ferretti, V. Pinchetti, M. Fanciulli, S. Brovelli, L. De Trizio and L. Manna, *J. Am. Chem. Soc.*, 2018, **140**, 12989-12995.
10. J. D. Majher, M. B. Gray, T. A. Strom and P. M. Woodward, *Chem. Mater.*, 2019, **31**, 1738-1744.
11. W. Lee, D. Choi and S. Kim, *Chem. Mater.*, 2020, **32**, 6864–6874.
12. P. Han, X. Zhang, C. Luo, W. Zhou, S. Yang, J. Zhao, W. Deng and K. Han, *ACS Central Sci.*, 2020, **6**, 566-572.